Asian Journal of Current Research in Clinical Cancer
ISSN: 3062-4444
2025, Volume 5, Issue 1, Page No: 81-92

Available online at: www.galaxypub.co/page/journals

Galaxy Publication

Galaxy Publication

Bile Acid Receptor FXR Agonism with Ocaliva Reduces Tumor Burden and MYC Signaling in Preclinical TNBC

I. Popovici[1*], C. Dumitru[1], V. Munteanu[1]

[1]Department of Oncology, School of Medicine, University of Chisinau, Chisinau, Moldova.

***E-mail** ✉ chisinau.onc.75@gmail.com

Received: 14 November 2024; **Revised:** 28 February 2025; **Accepted:** 05 March 2025

ABSTRACT

Bariatric procedures have been linked to better prognoses in several cancers, including breast cancer (BC), though the biological drivers of this benefit remain unclear. We proposed that the rise in circulating bile acids observed after bariatric surgery could play a role in enhanced BC outcomes. Individuals whose tumors showed elevated levels of the bile acid-responsive receptor FXR had improved survival in specific aggressive BC phenotypes. FXR, a nuclear receptor activated primarily by endogenous bile acids, was therefore selected as a therapeutic target. We hypothesized that stimulating FXR with an FDA-approved agonist might yield anti-neoplastic effects. Using both cell-based systems and animal models, we assessed whether pharmacological activation of FXR suppresses tumor behavior. Administration of the bile acid analog Obeticholic acid (OCA; INT-747; commercially "Ocaliva") markedly curtailed tumor growth and overall disease burden in a preclinical BC setting. Transcriptomic profiling of OCA-treated mouse tumors uncovered distinct gene expression differences relative to controls, including a notable reduction in MAX (MYC-associated factor X), a transcription factor that cooperates with MYC. Gene set enrichment analysis (GSEA) confirmed a significant suppression of the Hallmark MYC Target V1 gene ensemble following OCA exposure. Across multiple human and murine BC cell lines, FXR stimulation produced dose-dependent decreases in proliferation, motility, and cell viability. By contrast, synthetic activation of TGR5 (GPBAR1), another common bile acid receptor responsive mainly to secondary bile acids, showed no meaningful influence on cancer cell behavior. Altogether, activating FXR with a primary-bile-acid mimetic such as OCA exerts strong anti-tumor activity, seemingly by limiting growth and migration while reducing viability. These data highlight FXR as a potential tumor-suppressive target with relevance for personalized BC therapies.

Keywords: Nuclear hormone receptor, Bile acid receptor, Agonist, FXR, TGR5, Triple-negative breast cancer, TNBC

How to Cite This Article: Popovici I, Dumitru C, Munteanu V. Bile Acid Receptor FXR Agonism with Ocaliva Reduces Tumor Burden and MYC Signaling in Preclinical TNBC. Asian J Curr Res Clin Cancer. 2025;5(1):81-92. https://doi.org/10.51847/Kv9qA56ngW

Introduction

Breast cancer (BC) remains the most frequently diagnosed cancer among women and continues to be the top cause of cancer-related death. Since the mid-2000s, annual incidence among females has risen by roughly 0.5% per year [1]. Microbial metabolites—including bile acids—may influence tumor progression [2, 3]. Prior studies indicate that BC patients often exhibit reduced systemic levels of primary bile acids when compared with non-cancer controls [2, 4]. We reasoned that restoring or mimicking such primary bile acid signaling pharmacologically might provide therapeutic benefit. However, the contribution of microbiome-derived metabolites to BC biology remains insufficiently characterized [3], necessitating deeper investigation into bile acid-mediated pathways.

The principal human primary bile acids are cholic acid (CA) and chenodeoxycholic acid (CDCA) [2, 5]. Through microbial dehydroxylation or deconjugation at the 7α/7β position, these are converted to secondary bile acids, including lithocholic acid (LCA) and deoxycholic acid (DCA) [2]. Primary bile acids act largely through the nuclear receptor farnesoid X receptor (FXR; NR1H4), the predominant bile acid receptor (BAR) [2, 5-7]. FXR has previously been associated with anti-tumor functions in colorectal, bladder, and liver malignancies [8-11].

Our analyses further show that elevated FXR expression correlates with superior survival in ER− and basal-like BC cases, but not in luminal A or ER+ disease, suggesting an opportunity for subtype-specific therapeutic approaches.

Consequently, we examined BAR-related signaling using established mimetic agonists. Activation of FXR by Obeticholic acid (OCA; INT-747; Ocaliva) significantly impaired tumor expansion in vivo. In cell-based studies, OCA similarly suppressed proliferation and migration, while increasing cancer cell death. In contrast, targeting GPBAR1/TGR5—the membrane-bound bile acid receptor [2, 5]—failed to produce measurable anti-cancer effects. Thus, FXR activation appeared uniquely effective. Since bariatric surgery elevates bile acid pools, these results raise the possibility that such metabolic changes may contribute to enhanced cancer outcomes. Given that OCA is already FDA-approved for primary biliary cholangitis (PBC), repurposing it for cancer-related trials may be readily achievable.

Materials and Methods

Reagents

Unless otherwise specified, all chemicals were sourced from Sigma-Aldrich (St. Louis, MO, USA). Obeticholic acid (OCA; INT-747; Cat. HY-12222, MedChemExpress, Monmouth, NJ, USA), the TGR5 agonist INT-777 (Cat. HY-15677, MedChemExpress), and Paclitaxel ("Ptax"; Cat. N88686, AstaTech, Bristol, PA, USA; HY-B0015, MedChemExpress) were used for both animal and cell-based studies. Antibodies were obtained from Abcam, Invitrogen, and Proteintech, including polyclonal rabbit GPCR TGR5 (AB72608, Abcam), polyclonal rabbit NR1H4/FXR (AB235094, Abcam), polyclonal rabbit FXR (PA5-40755, Invitrogen), and monoclonal mouse GAPDH (60004-1-Ig, Proteintech®, Rosemont, IL, USA).

Cell Lines and media

E0771-luciferase (E0771-luc [12]) and 4T1 murine BC lines were acquired from ATCC and cultured in RPMI-1640 (Corning, Tewksbury, MA, USA) supplemented with 10% FBS (Gibco, Waltham, MA, USA), 1% penicillin/streptomycin, and 1% GlutaMAX. Human BC-related lines—MCF7, MDA-MB-231, SUM159 (gift from T. Seagroves), THP-1, and Huh7 (gift from A. Bajwa)—were grown in complete DMEM (Gibco) enriched with 10% FBS, 1% GlutaMAX, 2 mM MEM non-essential amino acids, 1 mM sodium pyruvate, and 1% penicillin/streptomycin. All cultures were maintained under sterile conditions at 37 °C with 5% CO_2. Mycoplasma status was routinely confirmed using the MycoAlert detection kit (Cat. LT07-318, Lonza, Basel, Switzerland). Cells were passaged at sub-confluence, and subculturing was restricted to the 10th passage for each line.

Proliferation assay

Proliferation of human SUM159 and MDA-MB-231 breast cancer cells, along with murine E0771 cells, was quantified using the IncuCyte S3 live-cell imaging platform (Sartorius AG, Göttingen, DE, Germany). SUM159 and MDA-MB-231 cultures were plated into 96-well plates at 1250 cells/well in 100 µL of full medium, whereas E0771 cells were seeded at 1000 cells/well in the same volume. After an overnight period to allow attachment, 10 µL of FXR or TGR5 agonists (OCA/INT-747 or INT-777) were added in a concentration-dependent series (1 µM, 10 µM, 50 µM, 100 µM) together with paclitaxel (Ptax) as the positive control at its designated doses. Confluency (%) was measured every 6 h over a 72 h period. Data represent n = 3-4 independent experiments with n = 4-8 wells per condition.

Cell viability assay

Cell survival was evaluated at 64 h using the Vybrant MTT assay kit (Molecular Probes, Eugene, OR). A 12 mM MTT stock was created in sterile PBS, and 10 µL was dispensed into each well. Following a 4 h incubation at 37 °C, 100 µL of SDS-HCl solution was added, and plates were incubated for another 4 h at 37 °C. Optical density was read at 570 nm using the Cytation 5 multimode imaging reader (BioTek, Winooski, VT, USA). Results represent n = 3 biological repeats with n = 4 technical replicates.

Migration assay

Cell motility was assessed via scratch-wound analysis on the IncuCyte S3 system. SUM159 and MDA-MB-231 TNBC cells were plated at 7500 cells/well in 96-well plates. When cultures reached 90% confluence, wounds

were introduced using the IncuCyte WoundMaker (Sartorius AG). Wells were rinsed twice with complete medium, and cells were maintained in 1% FBS during treatment with either OCA (0, 10, 50, 100 μM) or INT-777 (0, 1, 10, 50, 100 μM). Imaging continued for 66-78 h, and Relative Wound Density (%) was recorded every 6 h. Experiments include N = 3 biological replicates and n = 4-8 technical replicates.

Western immunoblot

Cells were grown to sub-confluent levels and lysed using RIPA buffer (Cat. 20188, EMD Millipore, Burlington, MA, USA) following established protocols [13-15]. Lysates were freeze-thawed, vortexed in 1× RIPA, and centrifuged at 12, 000× g for 10 min at room temperature. Protein concentrations were measured using the Rapid Gold BCA assay (Cat. A53225, PierceTM, Appleton, WI, USA). Eighty μg of total protein was loaded onto 12% SDS-PAGE gels and electrophoresed at 120 V for 45 min, followed by transfer to PVDF membrane (Invitrogen) overnight at 4 °C. Blots were incubated with anti-FXR and anti-TGR5 (1:2000, overnight), with GAPDH (1:5000, 1 h) as the loading control.

Xenograft model

All procedures were approved by the UTHSC IACUC (protocol #23-0432). Mice were housed on a 12 h light/dark schedule with standard breeder chow. MDA-MB-231 cells resuspended in serum-free DMEM were mixed at a 1:1 ratio with Matrigel (Product 354234, Corning®, Tewksbury, MA) and implanted into N = 30 female NSG mice (12-13 weeks old). A total of 5×10^5 cells in 100 μL (final Matrigel 4.5 mg/mL) were injected into the right 4th mammary fat pad. Animals were examined three times weekly until tumors reached 80-150 mm^3, measured via digital calipers. Mice were randomized into three cohorts:

- Vehicle (40% DMSO, 60% PEG; n = 8)
- OCA (30 mg/kg, n = 7)
- Ptax (10 mg/kg, n = 6)

Vehicle and OCA were administered daily by gavage; Ptax was given intraperitoneally three times per week. Tumor volume was calculated using the formula ($width^2 \times length / 2$) [13, 14, 16]. Body mass was recorded every other day. At the endpoint, mice were euthanized, tumors excised, weighed, photographed, and snap-frozen.

In silico analysis

Overall survival associations were evaluated using the Kaplan-Meier Plotter resource (kmplot.com) [17]. This tool integrates datasets from GEO [18], EGA [19, 20], and TCGA [21-23] as described by Gyorffy [24]. Analyses included NR1H4 (FXR) and MAX transcripts using the RNAseq dataset (IDs: nr1h4 and MAX). The follow-up criterion "all" was applied to include the full available time span. Sub-analyses for ER+, ER−, luminal A (PAM50), and basal-like TNBC used sample sizes of 2575, 214, 1504, and 309, respectively. No filters were applied for treatment type, trichotomization, or custom cutoffs; "auto select best cutoff" remained enabled. This feature evaluates all potential thresholds between upper and lower quartiles and applies Benjamini-Hochberg corrections for FDR [25].

Cutoff values were:

- NR1H4: ER+ / ER− = −3.0; luminal A = −2.94; basal-like = −2.61
- MAX: ER+ = 5.54; ER− = 5.08; luminal A = 5.54; basal-like = 4.99

Figures show hazard ratios (HRs), 95% confidence intervals, and log-rank p-values. Red curves indicate high expression; black curves denote low expression.

RNA-Seq and pathway analysis of MDA-MB-231 tumors

Tumor specimens from vehicle-treated animals (n = 7) and those receiving OCA (n = 6) were processed for RNA extraction using the RNeasy Mini Kit (#74104, Qiagen). RNA quality was examined on an Agilent TapeStation, and only samples exceeding a RIN of 6.0 proceeded to library construction. mRNA libraries were prepared for the Illumina workflow and sequenced at Azenta using a HiSeq setup, generating 2 × 150 bp reads.

Fastq files obtained from the HiSeq run were inspected with FastQC. Reads were aligned to the human genome reference hg38 (Gencode v45) with STAR [26], and the resulting aligned files were arranged via SAMtools [27]. Quantification of transcript abundance was performed using Salmon [28]. Gene-level ENSENBL counts were

imported into R version 4.3.1 [29], and tximport [30] was used to incorporate Salmon quantification files for differential expression analysis conducted in DESeq2 [31]. Differentially expressed genes (DEGs) were identified using an adjusted p-value cutoff of < 0.1. Regularized log (rlog) transformation from DESeq2 was applied for visualization and downstream steps. Heatmaps were produced with the ComplexHeatmap package [32], where gene rows were clustered using complete linkage and samples were grouped by treatment in a semi-supervised framework.

Genes found to be upregulated or downregulated were submitted to the DAVID portal [33, 34] to explore enriched pathways and gene ontology categories. Volcano plots displayed DEGs meeting statistical criteria: adjusted p-value ≤ 0.05 combined with log2|FC| ≥ 0.58.

Gene set enrichment analysis (GSEA) of MDA-MB-231 tumor RNA

GSEA (version 4.3.3) [35] was employed to identify enriched transcriptomic signatures. Input consisted of rlog-transformed data from 7 vehicle samples and 6 OCA samples. Gene set significance was evaluated using 1000 permutations, applying a false discovery rate (FDR) boundary of 0.25 (25%). Hallmark gene sets from the MSigDB Human Collection [36] served as the curated reference. For hallmark pathways, enrichment plots were shown when nominal p-values were below 0.05.

Statistical analysis

All numerical outcomes were reported as mean ± SEM using GraphPad Prism 10.0.2. Unless specified, analyses were based on at least three independent biological replicates. Comparisons between groups were made by Student's t-test or one-way ANOVA. Levels of statistical significance were represented using: p > 0.05 (), p > 0.01 (), p > 0.001 (), and p > 0.0001 (****).

Results and Discussion

Higher NR1H4 expression is associated with greater survival in patients with ER− and basal-like BC subtypes

Survival analyses were performed using KMPlotter with RNAseq datasets [25]. For ER+ cases, NR1H4 (FXR) expression did not noticeably influence overall survival **(Figure 1a)**. In luminal A tumors—the most common and least aggressive category—elevated NR1H4 expression was linked to a slight decrease in survival **(Figure 1b)**. By contrast, patients with ER-tumors exhibited improved survival when NR1H4 levels were higher **(Figure 1c)**. A similar survival trend appeared in basal-like tumors, including most TNBC cases **(Figure 1d)**, though without statistical significance. Altogether, elevated NR1H4 expression seemed most beneficial in the more aggressive disease subtypes.

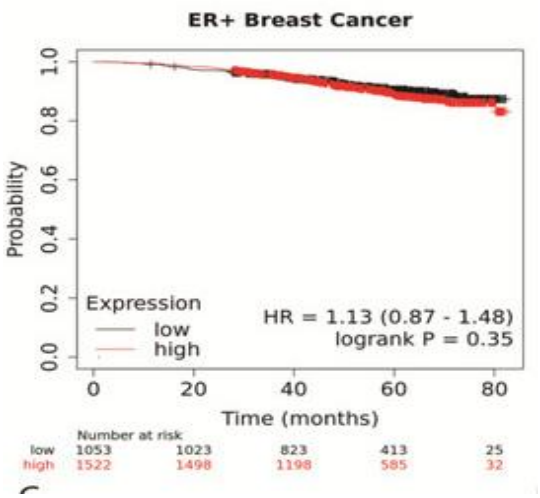

a)

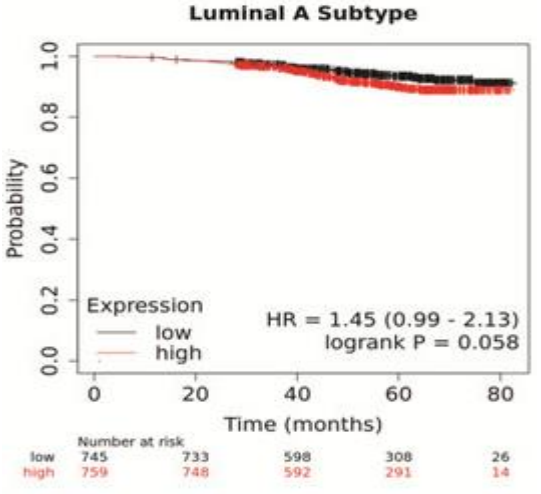

b)

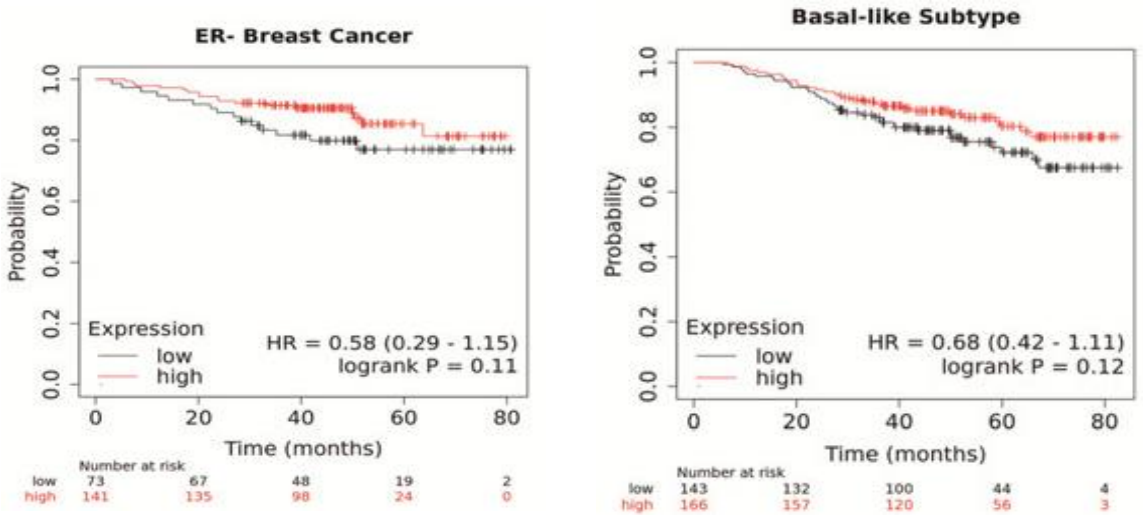

c) d)

Figure 1. NR1H4 expression patterns in various breast cancer categories. KMPlotter RNAseq-based survival analyses are shown for ER+ breast cancer (a), luminal A ER+ tumors (b), ER− cases (c), and basal-like TNBC (d). Patient counts at each monthly interval are provided for low- versus high-expression groups. Hazard ratios (HR) and log-rank P values compare high NR1H4 (red) to low NR1H4 (black).

FXR is expressed in human and murine triple-negative breast cancer cell lines

Because elevated NR1H4 correlated with improved survival in ER− and basal-like categories—commonly TNBC—we evaluated FXR protein presence in multiple cell systems. Western blot experiments showed detectable FXR in human breast cancer lines MDA-MB-231, MCF7, and SUM159. Across three blots, MDA-MB-231 (including high-passage cells) and MCF7 displayed the strongest FXR expression, whereas SUM159 showed comparatively low levels **(Figures 2a and 2b)**. THP-1 cells served as a low-FXR control, while Huh7 hepatocyte-like cells served as a positive reference. FXR expression was also observed in mouse-derived E0771 and 4T1 cells. Collectively, these findings indicate that the FXR protein is consistently present in diverse human and murine breast cancer models.

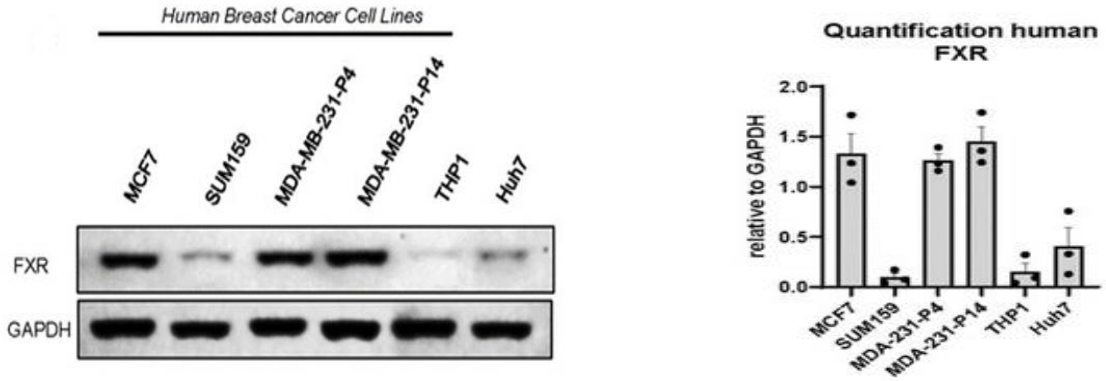

a) b)

Figure 2. FXR protein in breast cancer cell lines. (a) Endogenous FXR (56 kDa) was detected in MCF7 (ER+), SUM159, and MDA-MB-231 TNBC cells. MDA-MB-231 cells at passages 4 and 14 verified that FXR expression remains stable with additional passaging; experiments used passages <P10. THP-1 and Huh7 served as low and high FXR controls. GAPDH (37 kDa) was used for loading normalization. Images shown represent n = 3 blots. (b) Quantification was completed using ImageJ, with FXR normalized to GAPDH and plotted as mean −/+ SEM.

OCA administration suppressed TNBC tumor expansion in a xenograft setting

To assess whether stimulating FXR alters tumor development, we evaluated OCA in a TNBC xenograft system. Female NSG mice were inoculated with MDA-MB-231 cells, generating detectable tumors by day 36. Once

tumors reached 80 mm³, animals were stratified by tumor size and divided into treatment arms. Mice received either vehicle or the FXR agonist OCA, delivered orally once per day at 30 mg/kg in a 40% DMSO / 60% PEG mixture. A third group was given paclitaxel (Ptax) at 10 mg/kg, injected intraperitoneally three times weekly as a positive standard. None of the interventions altered body mass. OCA markedly slowed TNBC tumor expansion **(Figure 3a)** versus vehicle. As expected, Ptax also reduced tumor progression. At the study endpoint, OCA produced a 2.2-fold drop in tumor volume and a 2.6-fold decline in tumor weight relative to controls **(Figures 3b and 3c)**. Representative excised tumors are shown in **Figure 3d**. These results identify OCA as a strong in vivo inhibitor of breast tumor growth.

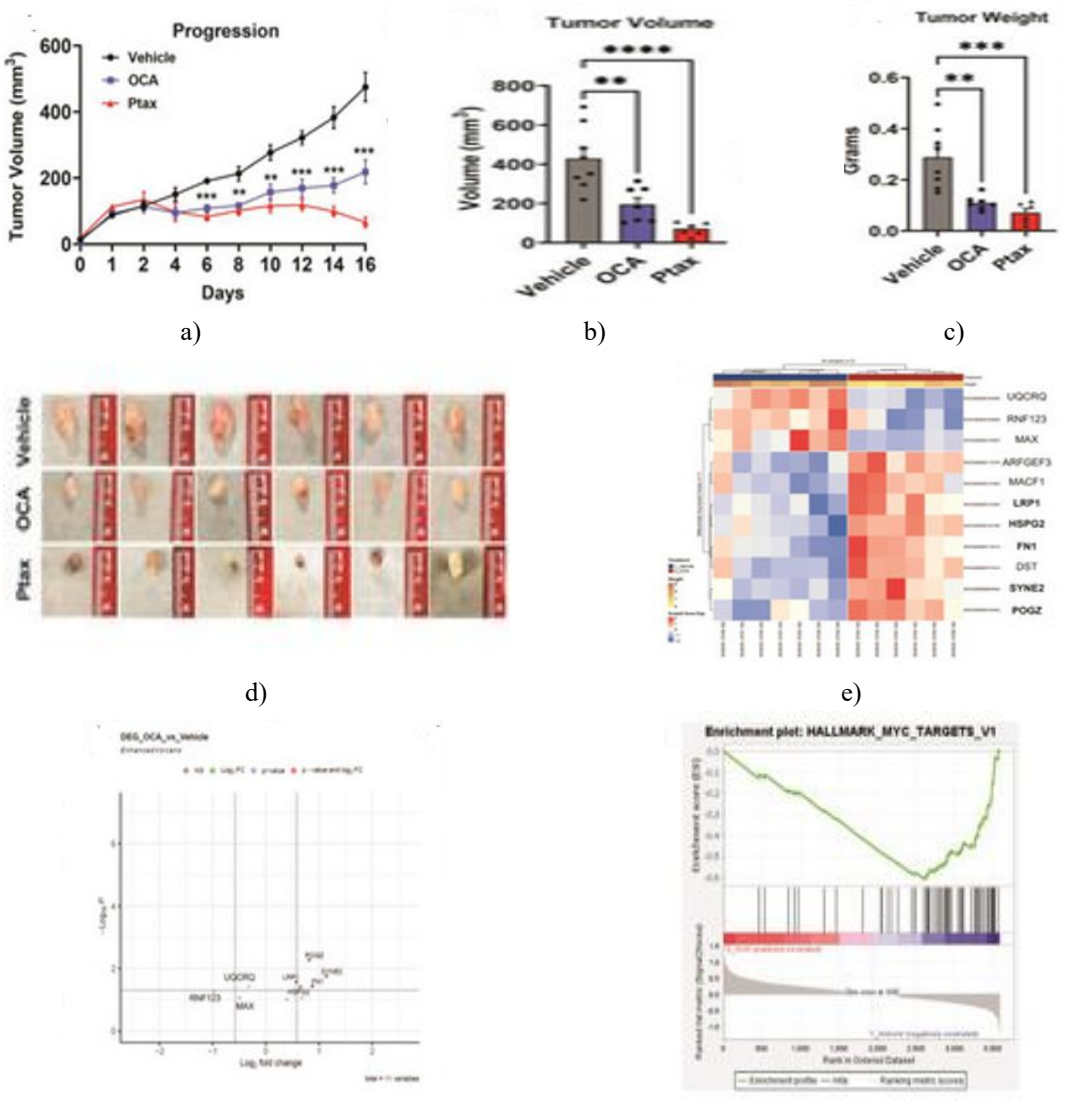

Figure 3. FXR activation by OCA diminished TNBC tumor load. Age-matched NSG females received MDA-MB-231 cells. Upon reaching 80 mm³, tumors were size-matched and treatments initiated. Vehicle or OCA (30 mg/kg) was delivered orally in 40% DMSO/60% PEG, and Ptax (10 mg/kg) was administered intraperitoneally three times weekly. Tumor measurements were taken daily via digital calipers. (a) Tumor trajectories for 16 days. (b, c) Final tumor volume and excised mass quantification. (d) Representative tumors from each cohort. (e) Semi-supervised RNA-seq heatmap comparing vehicle vs. OCA groups, with tumor mass and treatment indicated below the dendrogram. Highlighted genes correspond to significant hits in (f) the volcano plot. (g) GSEA enrichment curve for Hallmark_MYC_Targets_V1, nominal p = 0.025. Data shown as mean ± SEM, n = 6-8 animals per treatment. Significance assessed via one-way or two-way ANOVA using LSD (GraphPad Prism 10.1). Notation: p > 0.01, *p > 0.001, ****p > 0.0001.

Transcriptomic and GSEA profiling of OCA-treated TNBC tumors shows suppression of hallmark MYC target genes

RNA extracted from frozen tumors was used to identify transcriptional pathways linked to reduced tumor size in OCA-treated mice. Differentially regulated transcripts are presented in the heatmap **(Figure 3e)** and volcano visualization **(Figure 3f)**. OCA elevated DST (dystonin), a breast cancer-related tumor suppressor influencing adhesion [37], as well as POGZ, a regulator of genome stability and proper mitosis [38]. Conversely, OCA reduced MAX, a bHLHZ transcription factor that partners with MYC and is implicated in proliferation, glycolysis, and motility in breast cancer [39]. High MAX levels correspond to better survival in ER+ or luminal A cases (p = 0.0011, 0.0062), but correlate with poorer outcomes in ER− or basal-like TNBC (p = 0.008, 0.014). Thus, the OCA-driven decrease in MAX expression in TNBC likely confers a survival benefit. GSEA further indicated significant enrichment of Hallmark MYC Target V1 in control tumors, with downregulation after OCA exposure ((**Figure 3g)**, nominal p = 0.025).

FXR activation diminishes TNBC cell growth, survival, and motility

To delineate OCA's direct cellular effects, assays measuring proliferation, viability, and migration were performed using FXR activation at 0-100 µM. OCA caused a marked, dose-responsive reduction in proliferation of MDA-MB-231 cells; the 50 and 100 µM doses produced strong inhibition, with only slight effects at 10 µM **(Figure 4a)**. A similar dose-related pattern was observed for cell viability, which decreased significantly at higher concentrations and mirrored the 10 nM Ptax control **(Figure 4b)**. Migration, assessed via scratch assay, was unaffected at 10 µM, but substantially reduced at 50 and 100 µM **(Figures 4c and 4d)**. In a second TNBC line, SUM159, OCA produced the same dose- and time-linked decreases in proliferation, viability, and motility, with 100 µM being most effective. The murine line E0771 also displayed dose-dependent decreases in cell growth and viability, with 100 µM inducing extensive cell death, and migration was significantly impaired at 50 µM relative to DMSO. Collectively, FXR stimulation by this synthetic bile acid analogue exerts robust anti-cancer actions by limiting the survival, expansion, and migration of TNBC cells.

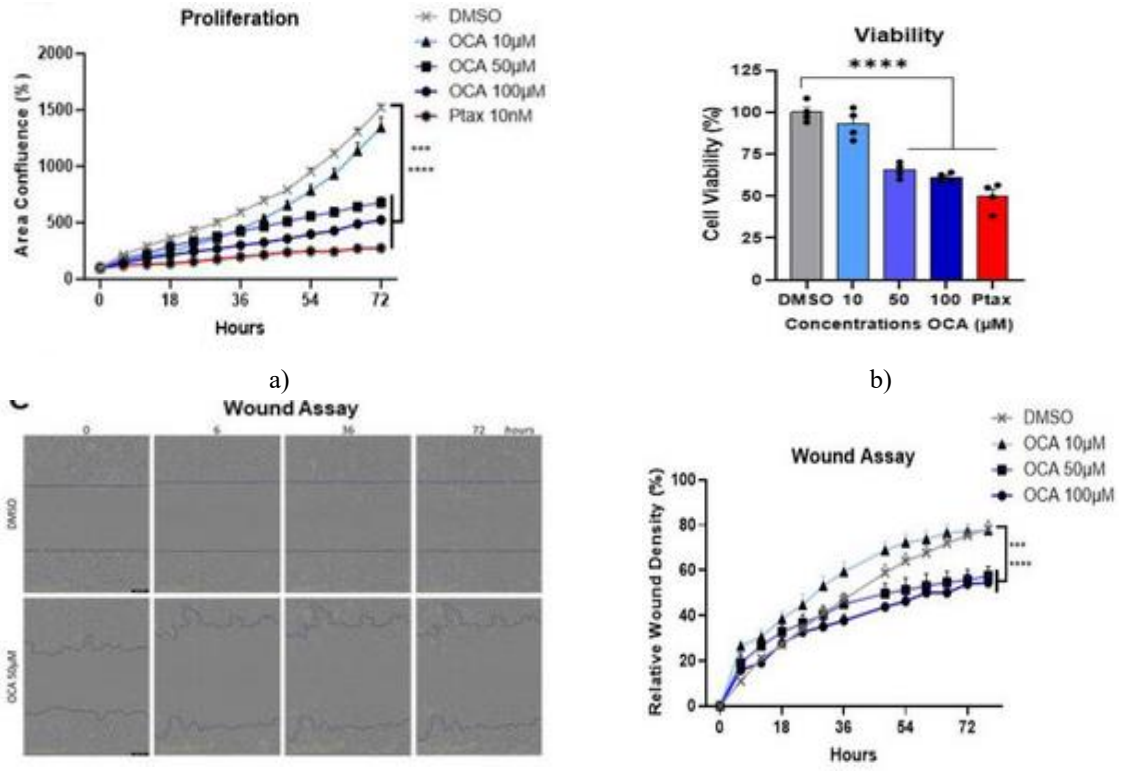

Figure 4. Effects of FXR activation on proliferation, viability, and migration. (a, b) MDA-MB-231 cells were plated at 1250 cells/well in 96-well plates and monitored with IncuCyte. Treatments used 0-100 µM OCA (INT-747), with 10 nM Ptax as a positive comparator. (a) Confluence (%) represents proliferation. (b) MTT-based viability at 64 h. (c, d) Migration quantified via IncuCyte scratch assay; cells plated at 7500 cells/well.

(c) Images at 0, 6, 36, and 72 h for DMSO and 50 μM OCA. (d) Relative wound density (%). Statistics: Fisher's LSD or one-way ANOVA; n = 4 technical replicates, representative of n = 3 biological replicates. Values shown as mean ± SEM. *** $p < 0.001$, **** $p < 0.0001$.

TGR5 bile acid receptor activation did not lessen triple-negative breast cancer cell growth, survival, or motility

To evaluate whether the anti-tumor responses were specific to FXR signaling, we also tested INT-777, a synthetic ligand for the bile acid receptor TGR5, for any comparable anti-cancer impact. TGR5 is abundantly expressed in human breast cancer cells. Activation of TGR5 in MDA-MB-231 and SUM159 cells failed to curb proliferation, viability, or movement. Likewise, INT-777 did not slow growth or reduce survival in murine E0771 cells and produced only minimal effects on migration. In several instances, higher doses of INT-777 even elevated proliferation and migration beyond levels seen with DMSO.

Bile acids have been implicated in modulating tumor behavior in several cancers, though their mechanistic role in TNBC has not been deeply examined before this work [3]. A reduction in breast cancer incidence after bariatric surgery [40] coincides with increased circulating bile acid concentrations observed post-operation [41], suggesting a possible therapeutic axis involving bile acid pathways. For this reason, we employed available synthetic bile acid analogs, including OCA, which is FDA-approved. The central conclusions of this study highlight a role for FXR signaling in breast cancer biology. Our results show that:

(i) individuals with elevated FXR levels exhibit improved survival specifically in ER− and basal-like tumors, but not in ER+ or luminal A disease;
(ii) both human and mouse breast cancer cell lines express FXR;
(iii) stimulating FXR with OCA slowed tumor growth in mice, potentially by suppressing MYC-associated transcriptional activity and reducing MAX expression;
(iv) OCA produced strong dose-dependent suppression of cell division, migration, and viability in vitro.

These effects appear to be specific to FXR, since the TGR5 agonist INT-777 yielded only weak inhibition of proliferation and viability and did not reduce migration. Prior reports likewise associate FXR expression with markers of favorable prognosis and independent prediction of survival [42, 43], though subtype-specific trends were not explored. Girisa *et al*. reviewed FXR involvement in several cancers [44], noting varied outcomes depending on the ligand used—often GW4064 (with some reports suggesting off-target effects [45]), CDCA, or guggulsterone. Notably, OCA (INT-747) had not been evaluated in those studies. The distinctive survival benefit in ER patients supports the possibility of subtype-tailored therapies utilizing bile acid receptor agonists. FXR is present in normal and malignant breast tissues and is associated with enhanced apoptosis [46]. It induces apoptosis in breast epithelial and cancer cells in vitro [47-49], consistent with our findings. Altogether, FXR activation may promote patient benefit through direct inhibition of cancer cell survival and movement. We propose that elevated bile acid metabolites—such as those increased after bariatric surgery—may enhance FXR signaling, thereby slowing neoplastic progression.

The microbiome may also influence cancer risk and development, though the field faces ongoing debate [3, 50, 51]. Microbial communities can alter levels of both host-derived and microbially generated metabolites, including bile acids [2]. Primary bile acids (1°)—such as cholic acid (CA), chenodeoxycholic acid (CDCA), and muricholic acid (MCA) in mice—are synthesized from cholesterol in the liver [2]. They are conjugated with glycine (GCA, GCDCA) or taurine (TCA, TCDCA) before entering the intestine. Microbes possessing 7-alpha-hydroxylase, including Clostridium cluster XIVa and Bacteroides, deconjugate primary bile acids, enabling conversion into secondary (2°) bile acids. These molecules can function as signaling hormones affecting inflammation, metabolism, and cancer through nuclear or membrane bile acid receptors. Patients with breast cancer have been reported to exhibit lower bile acid levels [5]. Interestingly, bile acids were discovered in human breast tissue decades ago, and oral BA administration was shown to preferentially accumulate there [52, 53]. Cook *et al*. further demonstrated that diet-modified bile acids appear in the breast tissue of non-human primates and do not necessarily mirror circulating levels [54]. These discoveries highlight the potential for future work exploring microbial and metabolite-driven influences on breast cancer development.

Obesity reshapes the gut microbiome and is linked with increased cancer incidence and mortality, including heightened breast cancer risk [3, 55]. Roughly two-thirds of U.S. adults are overweight or obese, with greater prevalence among women and higher rates in minority groups [56]. According to the WHO, obesity is defined as a BMI exceeding 30 kg/m² [57]. Bariatric surgery remains the most effective therapy for significant weight

reduction [55]. Several studies show that postoperative weight loss protects against ER− cancers, including TNBC [3, 40], and improves clinical outcomes [56]. Our recent work showed that bariatric surgery also diminished TNBC tumor growth in mice compared with obese sham-operated controls [14]. Elevations in bile acids after surgery may be one factor contributing to improved long-term cancer outcomes, including effects persisting 5-10 years after the procedure. Given how strongly obesity and weight loss influence microbial composition, and growing interest in microbial metabolites, it is plausible that bile acids or BAR activation contribute to the protective mechanisms suggested in this study.

Breast cancer subtypes are defined by ER, PR, and HER2 status; tumors lacking all three are classified as TNBC [2]. TNBC remains one of the most aggressive subtypes and lacks available targeted therapies because existing drugs primarily focus on these receptors. Limited targeted treatment options lead to higher recurrence, greater metastatic risk, and lower overall survival in TNBC patients [58, 59]. This unmet need underscores the importance of new targeted prevention or treatment strategies such as FXR activation. One cross-cancer immunotherapy study [60] reported that cases with high FXR (NR1H4) expression showed better survival following anti-PD-L1 therapy, although breast cancer was not included in that dataset [60]. While chemotherapy is still the primary option for TNBC, multiple immunotherapies have recently been approved. Yet not all patients respond, and some develop adverse events [61]. As immunotherapy use expands, examining how bile acids, FXR levels, or specific mutations shape therapeutic response may become increasingly significant.

Conclusion

Collectively, our findings indicate that FXR acts as a suppressor of tumor progression. Activating FXR led to pronounced reductions in aggressive cancer cell behavior and, in vivo, limited tumor growth. Overall, these data support the potential of FXR-targeted bile acid receptor agonists as promising therapeutic candidates with tumor-suppressive properties in breast cancer.

Acknowledgments: None

Conflict of Interest: None

Financial Support: None

Ethics Statement: None

References

1. Siegel RL, Miller KD, Wagle NS, Jemal A. Cancer statistics, 2023. CA Cancer J Clin. 2023;73(1):17–48.
2. Sipe LM, Chaib M, Pingili AK, Pierre JF, Makowski L. Microbiome, bile acids, and obesity: How microbially modified metabolites shape anti-tumor immunity. Immunol Rev. 2020;295(1):220–39.
3. Bohm MS, Sipe LM, Pye ME, Davis MJ, Pierre JF, Makowski L. The role of obesity and bariatric surgery-induced weight loss in breast cancer. Cancer Metastasis Rev. 2022;41(2):673–95.
4. Mikó E, Vida A, Kovács T, Ujlaki G, Trencsényi G, Márton J, et al. Lithocholic acid, a bacterial metabolite reduces breast cancer cell proliferation and aggressiveness. Biochim Biophys Acta Bioenerg. 2018;1859(11):958–74.
5. Režen T, Rozman D, Kovács T, Kovács P, Sipos A, Bai P, et al. The role of bile acids in carcinogenesis. Cell Mol Life Sci. 2022;79(5):1–39.
6. Chiang JY, Ferrell JM. Discovery of farnesoid X receptor and its role in bile acid metabolism. Mol Cell Endocrinol. 2022;548(1):111618.
7. Schumacher JD, Guo GL. Pharmacologic Modulation of Bile Acid-FXR-FGF15/FGF19 Pathway for the Treatment of Nonalcoholic Steatohepatitis. Handb Exp Pharmacol. 2019;256(1):325–57.
8. Huang X, Fan M, Huang W. Pleiotropic roles of FXR in liver and colorectal cancers. Mol Cell Endocrinol. 2022;543:111543.
9. Kao CC, Lai CR, Lin YH, Chen TM, Tsai YL, Tsai WC, et al. GW4064 inhibits migration and invasion through cathepsin B and MMP2 downregulation in human bladder cancer. Chem Interact. 2024;389:110869.

10. Golonka RM, Yeoh BS, Saha P, Tian Y, Chiang JY, Patterson AD, et al. Sex Dimorphic Effects of Bile Acid Metabolism in Liver Cancer in Mice. Cell Mol Gastroenterol Hepatol. 2024;17(5):719–35.
11. Stofan M, Guo GL. Bile Acids and FXR: Novel Targets for Liver Diseases. Front Med. 2020;7(544):544.
12. Pingili AK, Chaib M, Sipe LM, Miller EJ, Teng B, Sharma R, et al. Immune checkpoint blockade reprograms systemic immune landscape and tumor microenvironment in obesity-associated breast cancer. Cell Rep. 2021;35(12):109285.
13. Chaib M, Sipe LM, Yarbro JR, Bohm MS, Counts BR, Tanveer U, et al. PKC agonism restricts innate immune suppression, promotes antigen cross-presentation and synergizes with agonistic CD40 antibody therapy to activate CD8+ T cells in breast cancer. Cancer Lett. 2022;531:98–108.
14. Sipe LM, Chaib M, Korba EB, Jo H, Lovely MC, Counts BR, et al. Response to immune checkpoint blockade improved in pre-clinical model of breast cancer after bariatric surgery. eLife. 2022;11:e79143.
15. Simon SE, Ahmed U, Saad SM, Anwar A, Khan KM, Tan EW, et al. New synthetic phenylquinazoline derivatives induce apoptosis by targeting the pro-survival members of the BCL-2 family. Bioorg Med Chem Lett. 2022;67:128731.
16. Chaib M, Holt JR, Fisher EL, Sipe LM, Bohm MS, Joseph SC, et al. Protein kinase C delta regulates mononuclear phagocytes and hinders response to immunotherapy in cancer. Sci Adv. 2023;9(1):eadd3231.
17. Győrffy B, Lanczky A, Eklund AC, Denkert C, Budczies J, Li Q, et al. An online survival analysis tool to rapidly assess the effect of 22,277 genes on breast cancer prognosis using microarray data of 1,809 patients. Breast Cancer Res Treat. 2009;123(1):725-31.
18. Clough E, Barrett T, Wilhite SE, Ledoux P, Evangelista C, Kim IF, et al. NCBI GEO: Archive for gene expression and epigenomics data sets: 23-year update. Nucleic Acids Res. 2023;52(D1):D138-44.
19. Chang A, Jeske L, Ulbrich S, Hofmann J, Koblitz J, Schomburg I, et al. BRENDA, the ELIXIR core data resource in 2021: New developments and updates. Nucleic Acids Res. 2021;49(D1):D498-508.
20. Drysdale R, Cook CE, Petryszak R, Baillie-Gerritsen V, Barlow M, Gasteiger E, et al. The ELIXIR Core Data Resources: Fundamental infrastructure for the life sciences. Bioinformatics. 2020;36(11):2636-42.
21. Gao J, Aksoy BA, Dogrusoz U, Dresdner G, Gross BE, Sumer SO, et al. Integrative Analysis of Complex Cancer Genomics and Clinical Profiles Using the cBioPortal. Sci Signal. 2013;6(269):pl1.
22. Cerami E, Gao J, Dogrusoz U, Gross BE, Sumer SO, Aksoy BA, et al. The cBio cancer genomics portal: An open platform for exploring multidimensional cancer genomics data. Cancer Discov. 2012;2(5):401-4.
23. de Bruijn I, Kundra R, Mastrogiacomo B, Tran TN, Sikina L, Mazor T, et al. Analysis and Visualization of Longitudinal Genomic and Clinical Data from the AACR Project GENIE Biopharma Collaborative in cBioPortal. Cancer Res. 2023;83(17):3861-7.
24. Győrffy B. Survival analysis across the entire transcriptome identifies biomarkers with the highest prognostic power in breast cancer. Comput Struct Biotechnol J. 2021;19(1):4101-9.
25. Lánczky A, Győrffy B. Web-Based Survival Analysis Tool Tailored for Medical Research (KMplot): Development and Implementation. J Med Internet Res. 2021;23(10):e27633.
26. Dobin A, Davis CA, Schlesinger F, Drenkow J, Zaleski C, Jha S, et al. STAR: Ultrafast universal RNA-seq aligner. Bioinformatics. 2013;29(1):15-21.
27. Danecek P, Bonfield JK, Liddle J, Marshall J, Ohan V, Pollard MO, et al. Twelve years of SAMtools and BCFtools. GigaScience. 2021;10(2):giab008.
28. Patro R, Duggal G, Love MI, Irizarry RA, Kingsford C. Salmon provides fast and bias-aware quantification of transcript expression. Nat Methods. 2017;14(4):417-9.
29. R Foundation. R Foundation for Statistical Computing; Vienna, Austria; 2014.
30. Soneson C, Love MI, Robinson MD. Differential analyses for RNA-seq: Transcript-level estimates improve gene-level inferences. F1000Research. 2016;4:1521.
31. Love MI, Huber W, Anders S. Moderated estimation of fold change and dispersion for RNA-seq data with DESeq2. Genome Biol. 2014;15(12):550.
32. Gu Z, Eils R, Schlesner M. Complex heatmaps reveal patterns and correlations in multidimensional genomic data. Bioinformatics. 2016;32(18):2847-9.
33. Sherman BT, Hao M, Qiu J, Jiao X, Baseler MW, Lane HC, et al. DAVID: A web server for functional enrichment analysis and functional annotation of gene lists (2021 update). Nucleic Acids Res. 2022;50(W1):W216-21.

34. Huang DW, Sherman BT, Lempicki RA. Systematic and integrative analysis of large gene lists using DAVID bioinformatics resources. Nat Protoc. 2009;4(1):44-57.
35. Subramanian A, Tamayo P, Mootha VK, Mukherjee S, Ebert BL, Gillette MA, et al. Gene set enrichment analysis: A knowledge-based approach for interpreting genome-wide expression profiles. Proc Natl Acad Sci U S A. 2005;102(43):15545-50.
36. Liberzon A, Birger C, Thorvaldsdóttir H, Ghandi M, Mesirov JP, Tamayo P. The Molecular Signatures Database Hallmark Gene Set Collection. Cell Syst. 2015;1(6):417-25.
37. Jain PB, Guerreiro PS, Canato S, Janody F. The spectraplakin Dystonin antagonizes YAP activity and suppresses tumourigenesis. Sci Rep. 2019;9:14554.
38. Siouda M, Dujardin AD, Dekeyzer B, Schaeffer L, Mulligan P. Chromodomain on Y-like 2 (CDYL2) implicated in mitosis and genome stability regulation via interaction with CHAMP1 and POGZ. Cell Mol Life Sci. 2023;80(7):1-19.
39. Guddeti RK, Pacharla H, Yellapu NK, Karyala P, Pakala SB. MORC2 and MAX contributes to the expression of glycolytic enzymes, breast cancer cell proliferation and migration. Med Oncol. 2023;40(8):1-11.
40. Feigelson HS, Caan B, Weinmann S, Leonard AC, Powers JD, Yenumula PR, et al. Bariatric Surgery is Associated with Reduced Risk of Breast Cancer in Both Premenopausal and Postmenopausal Women. Ann Surg. 2019;272(6):1053-9.
41. Wang W, Cheng Z, Wang Y, Dai Y, Zhang X, Hu S. Role of Bile Acids in Bariatric Surgery. Front Physiol. 2019;10:374.
42. Giaginis C, Karandrea D, Alexandrou P, Giannopoulou I, Tsourouflis G, Troungos C, et al. High Farnesoid X Receptor (FXR) expression is a strong and independent prognosticator in invasive breast carcinoma. Neoplasma. 2017;64(4):633-9.
43. Barone I, Vircillo V, Giordano C, Gelsomino L, Győrffy B, Tarallo R, et al. Activation of Farnesoid X Receptor impairs the tumor-promoting function of breast cancer-associated fibroblasts. Cancer Lett. 2018;437:89-99.
44. Girisa S, Henamayee S, Parama D, Rana V, Dutta U, Kunnumakkara AB. Targeting Farnesoid X receptor (FXR) for developing novel therapeutics against cancer. Mol Biomed. 2021;2(1):1-23.
45. Singh N, Yadav M, Singh AK, Kumar H, Dwivedi SKD, Mishra JS, et al. Synthetic FXR Agonist GW4064 Is a Modulator of Multiple G Protein-Coupled Receptors. Mol Endocrinol. 2014;28(5):659-73.
46. Swales KE, Korbonits M, Carpenter R, Walsh DT, Warner TD, Bishop-Bailey D. The Farnesoid X Receptor Is Expressed in Breast Cancer and Regulates Apoptosis and Aromatase Expression. Cancer Res. 2006;66(20):10120-6.
47. Baker P, Wilton J, Jones C, Stenzel D, Watson N, Smith G. Bile acids influence the growth, oestrogen receptor and oestrogen-regulated proteins of MCF-7 human breast cancer cells. Br J Cancer. 1992;65(4):566-72.
48. Giordano C, Barone I, Vircillo V, Panza S, Malivindi R, Gelsomino L, et al. Activated FXR Inhibits Leptin Signaling and Counteracts Tumor-promoting Activities of Cancer-Associated Fibroblasts in Breast Malignancy. Sci Rep. 2016;6:21782.
49. Giordano C, Catalano S, Panza S, Vizza D, Barone I, Bonofiglio D, et al. Farnesoid X receptor inhibits tamoxifen-resistant MCF-7 breast cancer cell growth through downregulation of HER2 expression. Oncogene. 2011;30(37):4129-40.
50. Sepich-Poore GD, Zitvogel L, Straussman R, Hasty J, Wargo JA, Knight R. The microbiome and human cancer. Science. 2021;371(6536):1331-40.
51. Gihawi A, Ge Y, Lu J, Puiu D, Xu A, Cooper CS, et al. Major data analysis errors invalidate cancer microbiome findings. mBio. 2023;14(1):e0160723.
52. Javitt N, Budai K, Raju U, Levitz M, Miller D, Cahan A. Breast-gut connection: Origin of chenodeoxycholic acid in breast cyst fluid. Lancet. 1994;343(8903):633-5.
53. Raju U, Levitz M, Javitt NB. Bile Acids in Human Breast Cyst Fluid: The Identification of Lithocholic Acid. J Clin Endocrinol Metab. 1990;70(4):1030-4.
54. Shively CA, Register TC, Appt SE, Clarkson TB, Uberseder B, Clear KY, et al. Consumption of Mediterranean versus Western Diet Leads to Distinct Mammary Gland Microbiome Populations. Cell Rep. 2018;25(1):47-56.e3.

55. Aminian A, Wilson R, Al-Kurd A, Tu C, Milinovich A, Kroh M, et al. Association of Bariatric Surgery with Cancer Risk and Mortality in Adults With Obesity. JAMA. 2022;327(24):2423-33.
56. Flegal KM, Kruszon-Moran D, Carroll MD, Fryar CD, Ogden CL. Trends in Obesity Among Adults in the United States, 2005 to 2014. JAMA. 2016;315(21):2284-91.
57. Kanny D, Liu Y, Brewer RD, Garvin WS, Balluz L. Vital Signs: Binge Drinking Prevalence, Frequency, and Intensity among Adults--United States, 2010. MMWR Morb Mortal Wkly Rep. 2012;61(1):14-9.
58. Kohler BA, Sherman RL, Howlader N, Jemal A, Ryerson AB, Henry KA, et al. Annual Report to the Nation on the Status of Cancer, 1975–2011, Featuring Incidence of Breast Cancer Subtypes by Race/Ethnicity, Poverty, and State. J Natl Cancer Inst. 2015;107(6):djv048.
59. Kuchenbaecker KB, EMBRACE Study, Neuhausen SL, Robson M, Barrowdale D, McGuffog L, et al. Associations of common breast cancer susceptibility alleles with risk of breast cancer subtypes in BRCA1 and BRCA2 mutation carriers. Breast Cancer Res. 2014;16(6):1-27.
60. Kovács SA, Fekete JT, Győrffy B. Predictive biomarkers of immunotherapy response with pharmacological applications in solid tumors. Acta Pharmacol Sin. 2023;44(10):1879-89.
61. Obidiro O, Battogtokh G, Akala EO. Triple Negative Breast Cancer Treatment Options and Limitations: Future Outlook. Pharmaceutics. 2023;15(6):1796.